The Concurrent Complementary Operators Method Applied to Two-Dimensional Time-Harmonic Radiation and Scattering Problems

Omar M. Ramahi, *Senior Member, IEEE*, Vijaya Chebolu, and Xin Wu

***Abstract*—The concurrent complementary operators method (C-COM) has recently been applied to time-harmonic solution of Maxwell equations in two-dimensional space. In this paper, we present the application of the C-COM to the problem of electromagnetic scattering by conducting cylindrical objects in two-dimensional spaces. We show that the C-COM can effectively annihilate surface waves that impinge on the boundary at or near grazing incidence. The effectiveness of the C-COM is due to the fact that its wave absorption mechanism is independent of the wave number. To demonstrate the effectiveness and robustness of the C-COM in time-harmonic simulation, we present several numerical experiments. A strong agreement is obtained between the C-COM solution and the reference solutions even when the computational boundary is positioned only a fraction of a wavelength from the scatterer's body. Furthermore, we present a numerical experiment that shows the behavior of C-COM when waves impinge on the outer boundary at oblique incidence.**

***Index Terms*—Complementary operators method (COM), finite-difference frequency-domain method, partial differential equations, scattering, time-harmonic simulation.**

I. Introduction

WHEN solving the radiation problem using a numerical procedure that is based on partial-differential equations, the computational domain needs to be not only finite in size but also as small as possible in order to minimize computational burdens. Significant efforts have been made in the past 20 years to find means to truncate computational domains without compromising the accuracy of the solution. (The engineering and computational science literature is replete with papers describing various mesh-truncation techniques; a representative sampling of these techniques can be found in [1]–[11] and references therein).

The complementary operators method (COM) was originally introduced as a mesh-truncation technique for open-region finite-difference time-domain (FDTD) simulations [10]. The strength of the COM is its ability to fully cancel the first-order reflections that arise when the computational domain is terminated with a boundary operator or absorbing boundary condition (ABC). This cancellation takes place by averaging two independent solutions to the problem. Each of these two solutions is obtained by imposing boundary operators that are complementary to each other. Two operators are considered complementary if their reflection coefficients are equal in magnitude but are 180° out of phase, not only analytically but also in the discrete or numerical domain. Therefore, the two solutions that are generated from each of the operators separately, when averaged, result in a solution that does not contain any of the first-order reflections.

The COM requires two independent solutions of the problem, which lead to doubling the operation count. Despite this additional overhead, the COM remains highly effective and efficient when compared to other available mesh-truncation techniques [10], [11]. This is primarily due to the fact that the COM allows the terminal boundaries to be positioned very close to the source of radiation. Despite the effectiveness of COM, eliminating two independent runs of the algorithm remains desirable as the overhead requirement of the simulation is reduced by one-half. The concurrent complementary operators method (C-COM) was introduced to eliminate the two simulations' requirements of the COM [11]. In the C-COM method, two complementary operators are applied concurrently in a single simulation, resulting in an appreciable increase in modeling efficiency. Furthermore, since the two complementary operators are applied within a region external to the working domain, the C-COM is effective when the scattering object includes nonlinear media [11].

In this paper, the theory of C-COM is extended to include time-harmonic (frequency domain) solution of the scattering problem. Although the frequency-domain and time-domain simulation are two different mathematical representations of a single physical phenomenon, the numerical solution's paradigm is not expected to be identical, as numerical errors are strongly dependent on the numerical scheme [12]. For this reason, complementary operators need to be numerically adapted to fit the particular numerical model under consideration, and especially, to ensure that the error cancellation mechanism remains valid.

In [13], the C-COM was applied to the beam propagation method, where it was found to yield results that are appreciably more accurate than other mesh-truncation techniques. In [14] the C-COM was applied to the problem of a source radiating

Manuscript received June 5, 2002; revised February 27, 2003. This work was supported in part by the U.S. Department of Defense MURI Program on Effects of Radiofrequency Pulses on Electronic Circuits and Systems under AFOSR Grant F496200110374 and in part by the CALCE Electronic Products and Systems Center and the Minta Marin Fund at the University of Maryland at College Park.

O. M. Ramahi is with the Mechanical Engineering Department, Electrical and Computer Engineering Department, and CALCE Electronic Products and Systems Center, University of Maryland, College Park, MD 20742 USA (e-mail: oramahi@calce.umd.edu).

V. Chebolu and X. Wu are with the Mechanical Engineering Department and CALCE Electronic Products and Systems Center, University of Maryland, College Park, MD 20742 USA.

Digital Object Identifier 10.1109/TAP.2004.823993

in free space. In this paper, we briefly review the theory of C-COM in time-harmonic simulation. Next, we present the application of C-COM in the finite-difference frequency-domain (FDFD) simulation of radiation and scattering problems. We show that the concurrent implementation of the COM in time domain translates to node averaging in the system matrix of the frequency-domain method. Finally, we present a set of numerical experiments that were carefully designed to test the performance of the C-COM, especially for evanescent waves and waves impinging on the computational boundary with near-grazing angles.

II. C-COM for Time-Harmonic Simulation

The development here will be demonstrated by solving the problem of radiation or scattering in two-dimensional space. The governing equation is the Helmholtz wave equation, which, for the case of TM-polarization, is given by

$$\nabla^2 E_Z + k^2 E_Z = 0 \tag{1}$$

where k is the wave number. (For the case of TE-polarization, E_z is replaced by H_z.) The field E_z corresponds to the scattered or total field. (The physical boundary conditions pertaining to the scattering object will be adjusted in accordance with the formulation used.)

Let us consider a computational boundary normal to the x axis and located at $x = a$. Furthermore, let us assume that the problem domain lies to the left-hand side of $x = a$. When the complementary operators are applied to this boundary in a frequency-domain model, the resultant two discrete-domain complementary operators are given by [12]

$$\{D_x B\}E_z = \left\{(I - S^{-1})B\right\} E_z = 0 \tag{2}$$

$$\{\overline{D_x} B\}E_z = \left\{(I + S^{-1})B\right\} E_z = 0 \tag{3}$$

where B is a boundary operator, I and S^{-1} are the identity and space shift discrete operators respectively, and Δx is the grid spacing. The corresponding reflection coefficients are given, respectively, by

$$R\{D_x B\} = -e^{jk,\Delta x} R\{B\} \tag{4}$$

$$R\{\overline{D_x} B\} = e^{jk,\Delta x} R\{B\} \tag{5}$$

where $R\{B\}$ is the reflection coefficient of the operator B and k_x is the wave number in the x direction. Notice that $R\{D_x B\}$ and $R\{\overline{D_x} B\}$ are precisely 180° out of phase and, hence, full complementariness is achieved analytically and numerically [12].

The boundary operator B above can be any analytical or even numerical boundary condition [15]. Previous work has shown that the Bayliss–Turkel (BT) series of operators offers very highly accurate and robust boundary conditions that yield asymptotic convergence in two-dimensional space and uniform convergence in three-dimensional space, as the order of the operator increases. In fact, it was found that the higher order BT operators can be implemented without approximations yielding high accuracy [16]. In this paper, the synthesis of complementary operators is based on the BT boundary conditions.

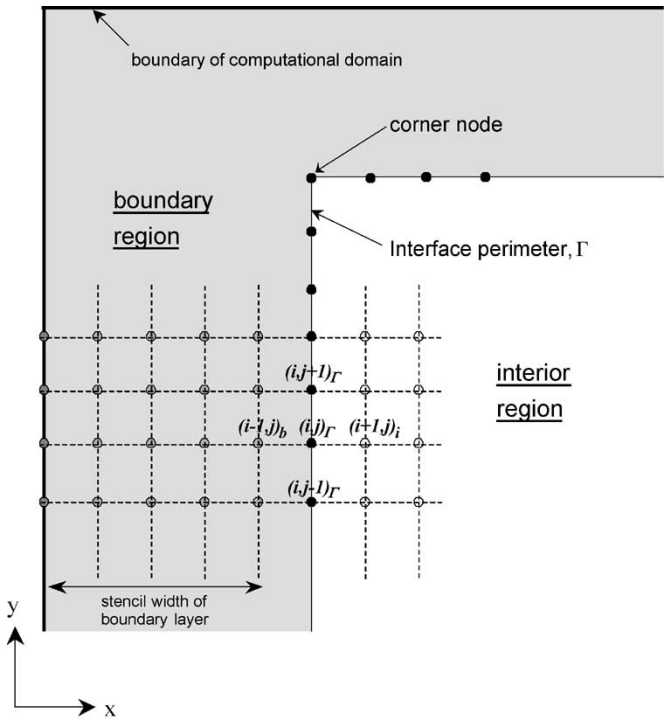

Fig. 1. The finite-difference frequency-domain grid highlighting the interior and boundary regions designated for the application of the C-COM. Also shown is the interface perimeter Γ, along which the fields from the boundary region are averaged.

For a planar (Cartesian) boundary, the Nth-order BT operator in frequency domain for a planar boundary is expressed as

$$B = (\partial_n + jk)^N \tag{6}$$

where $\partial_{\rm n}$ is the partial derivative of the field in the direction normal to the computational boundary. We will refer to the Nth-order BT operator as BTN. When the outer boundary is planar and coinciding with the Cartesian planes, (5) reduces to Higdon's boundary condition when it is applied in the frequency domain.

III. Implementation in Finite-Difference Simulations

The first step in the implementation of the FDFD method is to divide the computational region into grid. Following a procedure highly similar to that used in the implementation of the C-COM in time-domain simulation [11], we divide the computational domain (grid) into two nonoverlapping regions—a boundary region and an interior region—as shown in Fig. 1. The interior region includes all radiating or scattering objects, while the boundary region is an empty domain set up purely for computational purposes. To each field node in the boundary region we assign two field values E_z^1 and E_z^2. In the interior region we assign a single field value E_z to each node, as in conventional implementation. Next, we apply the second-order accurate finite-difference scheme to each node in the interior region as in standard implementation. For ease of illustration, we assume that the grid is uniform in the x and y directions with grid spacing of Δ. For clarity, we make the following designations: all interior nodes will be designated as $(i, j)_i$, all nodes lying within the boundary region will be designated as $(i, j)_b$, and all

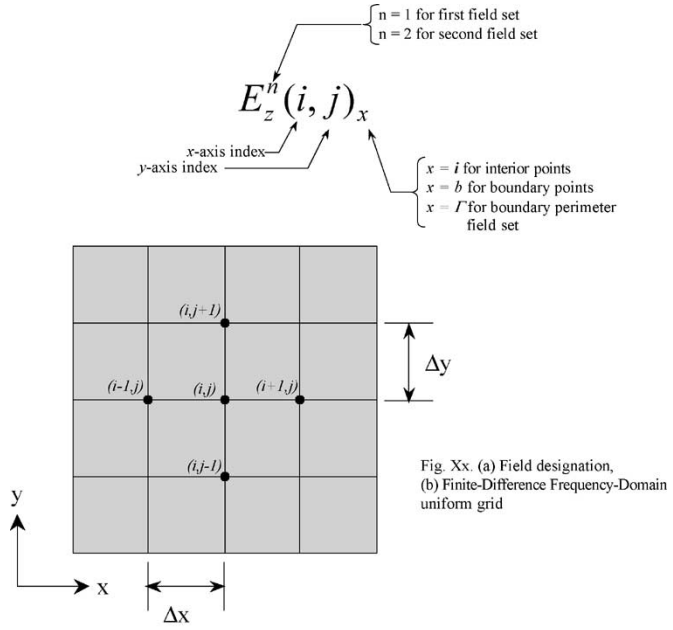

Fig. Xx. (a) Field designation, (b) Finite-Difference Frequency-Domain uniform grid

Fig. 2. FDFD grid showing fields locations and designation.

nodes lying on the interface perimeter Γ will be designated as $(i,j)_\Gamma$. A schematic of the FDFD grid and field designation is shown in Fig. 2.

Applying the FDFD scheme to the free-space Helmholtz equation at an interior node $(i,j)_i$, we have

$$E_z(i-1,j)_i + E_z(i+1,j)_i + E_z(i,j+1)_i + E_z(i,j-1)_i + (k^2\Delta^2 - 4)E_z(i,j)_i = 0. \quad (7)$$

In the boundary region, we apply the finite-difference equation to each set of fields designated by the superscripts 1 and 2. We have

$$E_z^1(i-1,j)_b + E_z^1(i+1,j)_b + E_z^1(i,j+1)_b + E_z^1(i,j-1)_b + (k^2\Delta^2 - 4)E_z^1(i,j)_b = 0 \quad (8)$$

$$E_z^2(i-1,j)_b + E_z^2(i+1,j)_b + E_z^2(i,j+1)_b + E_z^2(i,j-1)_b + (k^2\Delta^2 - 4)E_z^2(i,j)_b = 0. \quad (9)$$

The next step is the implementation of the complementary operators. The first operator D_x is applied to the set of fields denoted by E_z^1 and the second operator $\overline{D}_x$ is applied to the second set of fields denoted by E_z^2. More explicitly, we have

$$\{D_x B\}E_z^1 = 0 \quad (10)$$

$$\{\overline{D_x} B\}E_z^2 = 0. \quad (11)$$

The final step links the boundary and interior regions. This is accomplished by constructing an interface between the two regions. On the interface, the field values needed from the boundary region for the FDFD equation are obtained from the average values of E_z^1 and E_z^2. Let Γ be the interface perimeter between the boundary layer and the interior region. (The interior region is inclusive of Γ.) Let us focus on the left-hand-side segment of Γ shown in Fig. 1. On Γ, the update equation for the fields uses the average field values $(E_z^1 + E_z^2)/2$ from the left-hand side and E_z from the interior region. Thus, the finite difference equation for the fields on Γ is given by

$$\frac{1}{2}\{E_z^1(i-1,j)_b + E_z^2(i-1,j)_b\} + E_z(i+1,j)_i + E_z(i,j+1)_\Gamma + E_z(i,j-1)_\Gamma + (k^2\Delta^2 - 4)E_z(i,j)_\Gamma = 0. \quad (12)$$

Similar equations are applied on the other three sides of Γ. The FDFD equations for the corner nodes of the interior region are slightly different. For example, the finite difference equation for the upper left-hand corner node is given by

$$\frac{1}{2}\{E_z^1(i-1,j)_b + E_z^2(i-1,j)_b\} + E_z(i+1,j)_\Gamma + \frac{1}{2}\{E_z^1(i,j+1)_b + E_z^2(i,j+1)_b\} + E_z(i,j-1)_\Gamma + (k^2\Delta^2 - 4)E_z(i,j)_\Gamma = 0. \quad (13)$$

The width of the boundary region must be greater than the width of the stencil demanded by the differential operator used in the C-COM. For instance, if B is a third-order BT operator, then the order of the C-COM operation is four [i.e., a fourth-order derivative would be needed to implement (10) and (11)], and consequently, the width of the stencil needed will be five. This implies that the boundary region has to be at least six nodes wide.

The above methodology can be extended to annihilate reflections arising from the corner regions as in [10] and [11]. For this, four field values need to be allocated for each FDFD node in the boundary region. (The reader is referred to [10] and [11] for a discussion on the annihilation of reflections coming from the corners of the computational domain.)

In a manner consistent with the nomenclature used for the COM method [10], nth-order C-COM operation [employing an nth-order operator in (10) and (2)] will be denoted as $\mathrm{C-COM}n$. For this, the minimum width of the boundary region is $n+2$ nodes inclusive of the boundary node. Furthermore, we use two additional parameters to fully identify the methodology used in terms of doubling or quadrupling the fields in the boundary layer and its width. When the fields are *doubled* in the boundary region, resulting in the cancellation of side reflections only, we refer to the method as C-COM$n(2,W)$, where W indicates the width of the boundary layer. Similarly, when the fields are *quadrupled* in the boundary region, annihilating corner reflections, we refer to the method as C-COM$n(4,W)$.

The primary figure of merit for overhead calculation in an FDFD method is the number of unknowns needed for the system matrix. When implementing C-COM$n(2,W)$, for instance, the field storage within the boundary region is doubled. As an example, when using C-COM$n(2,W)$ in a computational domain of size $N \times M$, the additional number of unknowns required in comparison to traditional ABC implementation (such as Higdon's boundary conditions) would be the number of nodes in the boundary region, which equals $N \times W \times 2 + [M - (2 \times W)] \times W \times 2$. Therefore, the minimum number of additional unknowns is found by substituting $n+2$ for W to give $2(n+2)(N+M) - 4(n+2)^2$. Clearly, the

percentage increase in overhead diminishes as the size of the problem increases.

Finally, we note that implementing (12) and (13) within the system matrix is simple. The sparsity of the matrix system is not affected by (12) and (13). However, a good node-numbering scheme can be exploited if a banded matrix solver is employed. The node numbering scheme can also be exploited to increase the efficiency of highly optimal solvers that store only nonzero matrix elements as these schemes employ approximations and iterations that depend on the nodal distance of each two adjacent nodes.

IV. Numerical Validation

The validity, robustness, and accuracy of the C-COM procedure are demonstrated by considering several numerical experiments that involve radiating and scattering sources. In all cases considered, validation is made by comparison to either the analytical solution (where possible) or to the reference solution, which is considered here to be the numerical solution where the computational domain is taken to be very large such that the reflections coming from the outer boundary are very small.

In the first test, we design a numerical experiment to test the effectiveness of the C-COM on the absorption of waves incident on the boundary at different angles of incidence. (This experiment is similar to a test performed in [17, ch 7].) We consider a two-dimensional computational domain of 200 $\Delta \times 21\ \Delta$. In these numerical experiments, the grid will be uniform in the x and y directions with $\Delta = 0.05\ \lambda$. We place a current source at (20 Δ, 11 Δ) and position three monitor points, designated as MP1, MP2, and MP3, along a horizontal line coincidental with the source and at a distance from it of 1λ, 3λ, and 7λ, respectively. The field observed at each monitor point will be composed *predominantly* of the line-of-sight wave coming from the source (corresponding to the physically observed wave) and two equal-magnitude spurious waves that have made a single bounce off the computational boundary (specular reflection off the boundary). Notice that other waves are also received due to multiple reflections, but these have much lower magnitudes and are assumed to be negligible. The angles of reflection (as measured with respect to the normal) that correspond to the spurious waves observed at the monitor points are 45°, 72°, and 82°, corresponding to MP1, MP2, and MP3, respectively.

Let the exact field at each of the monitor points be E^{ex}. The computed field is approximately given by $E^{\mathrm{c-com}} = E^{\mathrm{ex}} + 2\,\delta$, where δ is the spurious reflection coming from one of the two top and bottom boundaries, as indicated in Fig. 3. The *approximate* normalized percentage error is then given by

$$\text{Normalized Error} = 100 \times \frac{\delta}{E^{\mathrm{ex}}} = \frac{1}{2}\left| 100 \times \frac{E^{\mathrm{ex}} - E^{\mathrm{c-com}}}{E^{er}} \right|. \tag{14}$$

The exact solution E^{ex} is obtained from the series solution. Notice that the exact solution includes numerical errors, which are not attributed to boundary condition reflections such as numerical dispersion. Clearly, a more accurate error analysis would entail generation of a *reference* solution (which would include numerical dispersion) obtained when the computational domain is made large enough such that any reflections from the boundary is negligible; however, due to the size of the domain already considered, this exercise would be numerically impractical.

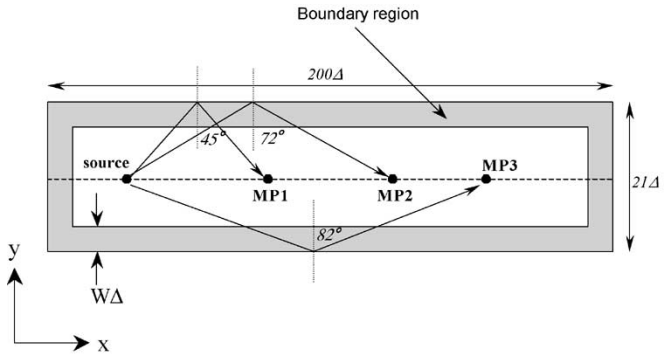

Fig. 3. Computational domain used to test the effect of different angles of incidence on the outer boundary.

TABLE I
Normalized Error at MP1, MP2, and MP3 as a Function of the Boundary Region Width W

Width of Boundary Region, W, in nodes	Error at MP1 (θ=45°)	Error at MP2 (θ=72°)	Error at MP3 (θ=82°)
6	0.32%	0.35%	6.14%
8	0.31%	0.19%	5.25%
9	0.29%	0.07%	4.98%

Table I shows the normalized error when using C-COM}4(2,W) for the three different monitor points. The error is observed to decrease with an increase in the width of the boundary region in a manner consistent with the theory of the C-COM as presented earlier for time-domain simulation [11]. Notice that the computational domain was kept constant while the boundary region was increased. These results further show that the suppression of reflections is very effective, especially for waves approaching the boundary at near-grazing incidence.

As a second experiment, we consider a simple problem intended to facilitate comparison between the C-COM solution and the solutions obtained from a recently published FDFD perfectly matched layer (PML) formulation [18]. We consider the problem of a point source radiating in free space. A 15 $\Delta \times 15\ \Delta$ core computational domain is chosen upon which additional grid layers will be added. The grid size will be chosen uniform in the x and y directions with $\Delta = 0.025\ \lambda$. The solution will be observed at the 15 grid points spanning the top of the core domain as indicated in Fig. 4. Fig. 5 shows the normalized error in the field obtained using the total-field-formulation FDFD-PML code, which incorporates an optimized conductivity profile and an eight-layer PML. (For details on the FDFD-PML formulation, the reader is referred to [18]; however, the results presented in this paper have been obtained directly from the authors of [18].) Note that the PML layers are added on each side to give a computational domain of 31 $\Delta \times 31\ \Delta$. Comparison is made to the C-COM3(2,5) solution in a computational domain of size 31 $\Delta \times 31\ \Delta$. For maximum efficiency in using C-COM3, the field averaging is performed only five nodes from

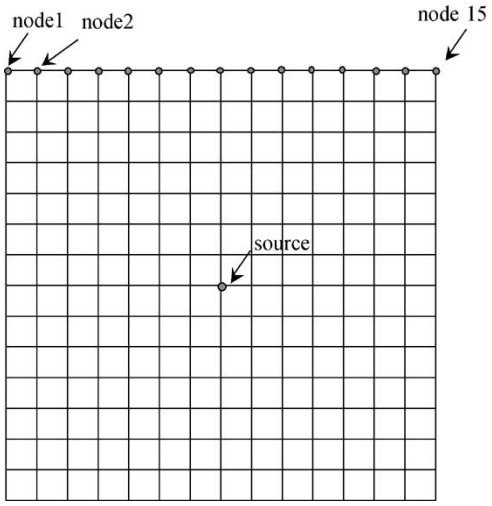

Fig. 4. Core FDFD computational domain used for the problem of a source radiating in free space. The observation contour is shown with the node numbering scheme corresponding to the solution presented in Figs. 5 and 6.

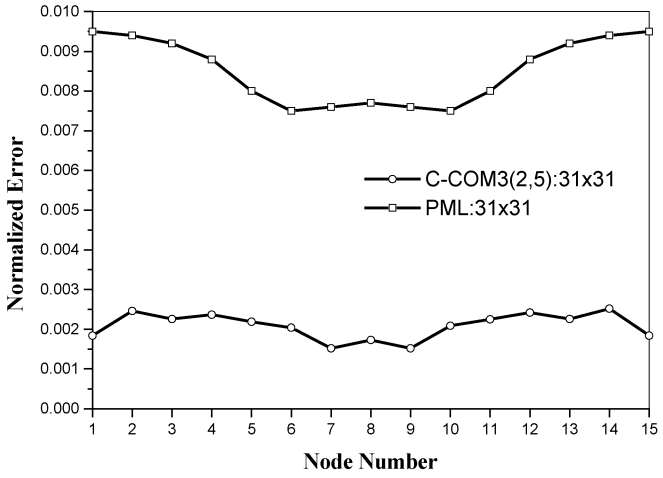

Fig. 5. Normalized error in the E-field at the top of the computational domain shown in Fig. 4 as obtained using an eight-layer PML and C-COM3(2,5), in a computational domain of size 31 Δ $\times$ 31 Δ.

the terminal boundary; hence, field-storage duplication is confined to the five-layer boundary region. Fig. 5 shows that for the fixed computational domain of size 31 $\Delta \times 31\ \Delta$, C-COM3(2,5) yields higher accuracy than the PML formulation of [18]. From Fig. 5, we observe that C-COM3(2,5) yields a maximum error of 0.0025 while the PML solution gives a maximum error of 0.0095.

The higher accuracy achieved by C-COM3(2,5) in the 31 $\Delta \times$ 31 Δ computational domain requires additional memory resources of approximately 50% in the number of unknowns of the system matrix for this *particular* problem. It should be noted, however, that for general problems of practical significance that would involve scattering objects, the area of field duplication is a small fraction of the total computational domain and, therefore, the increase in overhead arising from the C-COM application is less burdensome. Furthermore, because of the high-accuracy potential of the C-COM, it is expected that the computational boundary can be reduced in comparison to solutions using traditional boundary treatments. To demonstrate the potential of

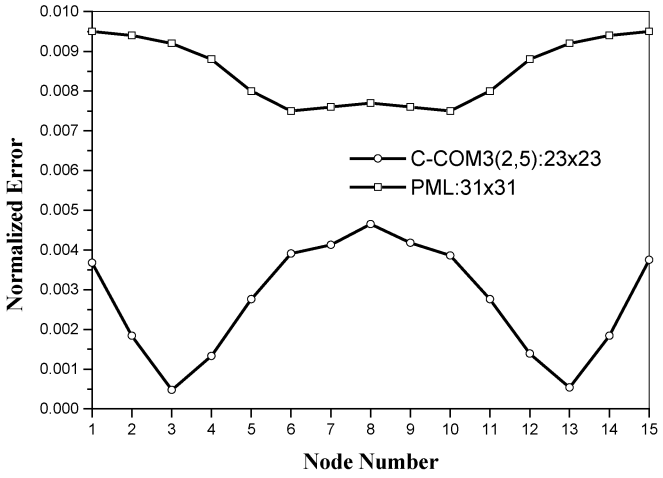

Fig. 6. Normalized error in the E-field at the top of the computational domain shown in Fig. 4 as obtained using eight-layer PML in a computational domain of size 31 Δ $\times$ 31 Δ and C-COM3(2,5) in a computational domain of size 23 Δ $\times$ 23 Δ.

the C-COM, a more stringent case is considered in which the computational domain is reduced to a size of 23 $\Delta \times 23\ \Delta$ while applying C-COM3(2,5). Fig. 6 shows a comparison between the FDFD-PML solution (eight-layer PML) where the total computational domain is 31 $\Delta \times 31\ \Delta$ and the C-COM3(2,5) solution in a computational domain of 23 Δ $\times$ 23 Δ. This time, however, we observe from Fig. 6 that the C-COM solution resulted in approximately 50% less maximum error in comparison to the FDFD-PML solution while yielding an FDFD system matrix having approximately 8% less number of unknowns than the FDFD-PML solution.

The FDFD-PML formulation is typically optimized for the angle of maximum absorption and conductivity profile, while the C-COM implementation does not call for any special problem-dependent adaptation or optimization. That is why we emphasize that the comparison between the FDFD-PML and the C-COM presented here is intended for the sole purpose of giving a preliminary qualitative assessment of computational resource requirements versus accuracy. A more comprehensive comparison will be the subject of a future publication.

Next, we turn to the problem of plane TM (transverse-magnetic, or E-wave) scattering by a 2.0 λ $\times$ 2.0 λ perfectly conducting square cylinder. The size of the computational domain is 54 $\Delta \times 54\ \Delta$. The grid will be chosen uniform in the x and y directions with $\Delta = 0.05\ \lambda$. This experiment is chosen in order to study the performance of C-COM in the shadow region of a scatterer where the scattered field has a relatively high magnitude in comparison to other regions around the scatterer. The outer boundary is positioned such that the separation between it and the conductor is 0.35λ. A total of 164 nodes span the observation contour, starting from the lower left-hand corner as shown in Fig. 7. Fig. 8(a) and (b) shows the magnitude of the scattered field on the observation contour for two different angles of incidence of $\phi = 0°$ and $\phi = 45°$. The accuracy of C-COM4(2,7) is observed to be quite satisfactory, especially in the shadow region of the scatterer.

For the next numerical experiment, we study the TM and TE scattering from a thin perfectly conducting rectangular

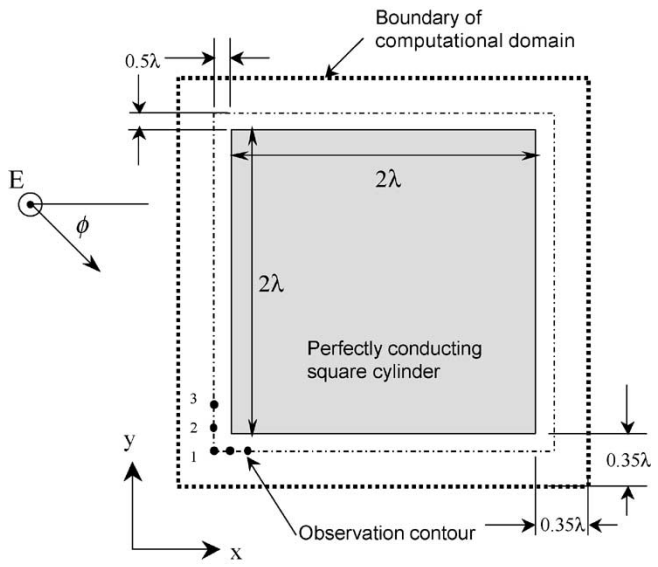

Fig. 7. Computational domain used for the problem of plane wave TM scattering from a perfectly conducting slab measuring 2.0 $\lambda \times 2.0\,\lambda$.

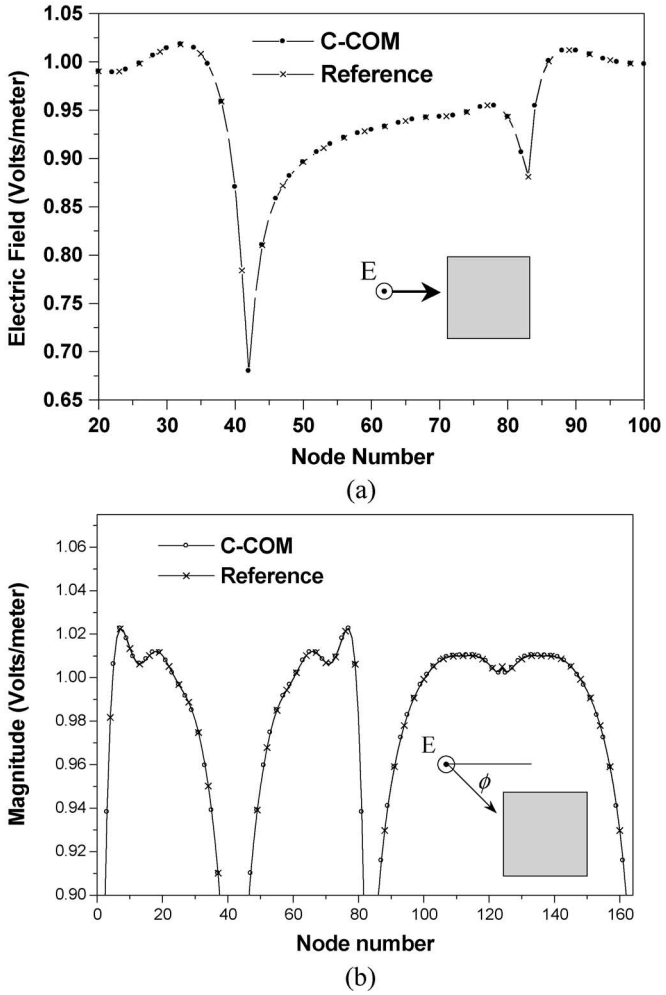

Fig. 8. Magnitude of the scattered field along Γ for the geometry shown in Fig. 7, the node numbering starts with the lower left-hand corner, as calculated using FDFD with C-COM4(2,7) (C-COM), and the reference solution (Reference), for two different angles of incidence (a) $\phi = 0.0°$, (b) $\phi = 45°$.

slab measuring 0.2 $\lambda \times 3\,\lambda$. The size of the computational domain is 77 $\Delta \times 21\,\Delta$. The outer boundary is positioned such

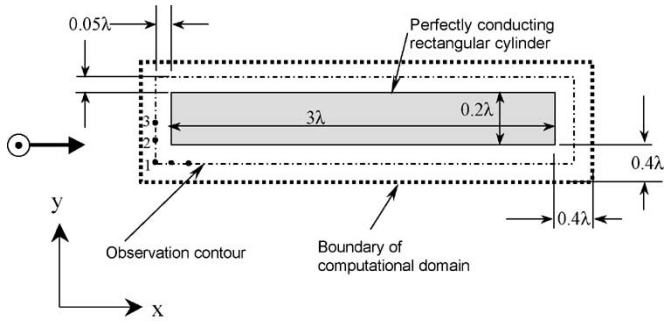

Fig. 9. Computational domain used for the problem of plane wave scattering from a perfectly conducting slab measuring 3 $\lambda \times 0.2\,\lambda$.

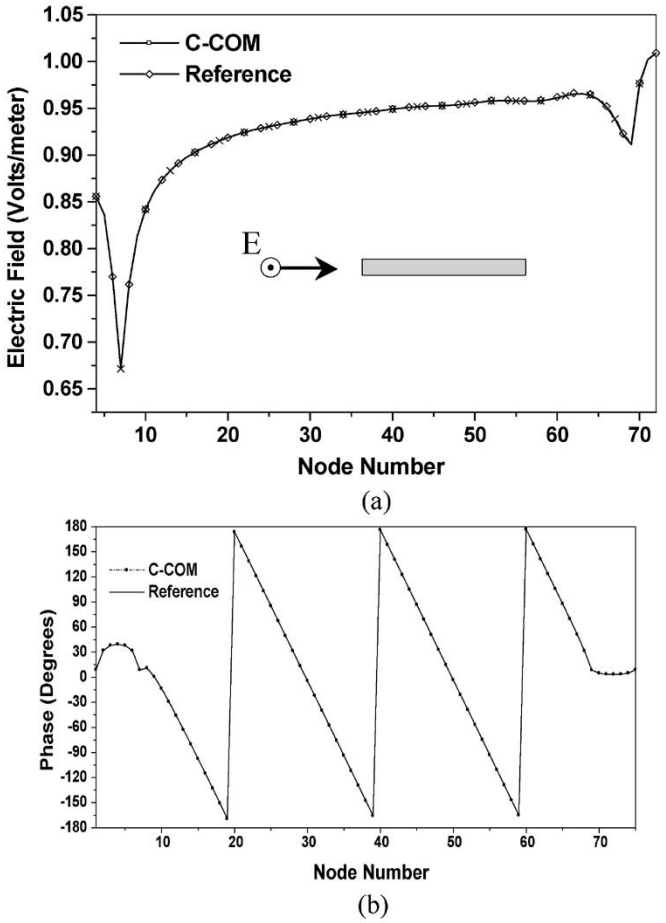

Fig. 10. Scattered field along Γ for plane wave incidence, TM-polarization (geometry shown in Fig. 7). The node numbering starts with the lower left-hand corner and proceeds clockwise. Because of symmetry, only filed points along the upper half of the contour are plotted. Field calculated using FDFD with C-COM4(2,7) (C-COM) and the reference solution (reference). (a) Magnitude and (b) phase.

that the separation between it and the conductor is 0.4λ, as illustrated in Fig. 9. Fig. 10(a) and (b) shows the magnitude and phase of the scattered field due to a TM plane wave incidence. The figures show the scattered field as calculated using the C-COM method and the reference solution for comparison at an observation contour Γ, as calculated using the FDFD method with C-COM4(2,7). A total of 136 nodes span the observation contour Γ. The numbering of the nodes starts at the lower left-hand corner and proceeds clockwise. Results are

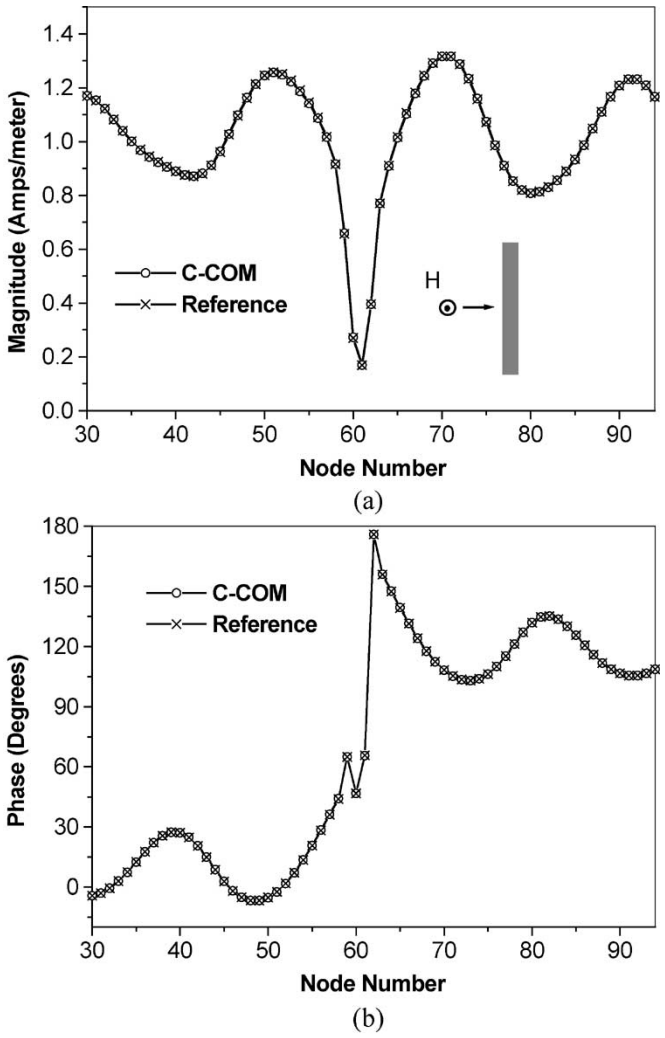

Fig. 11. Surface current density along the surface of a perfectly conducting slab for the case of broadside incidence, TE-polarization. Because of symmetry, only half of the surface span is considered. Node 30 corresponds to the middle of the left-hand-side surface. Nodes increase in number in the clockwise direction. (a) Magnitude and (b) phase.

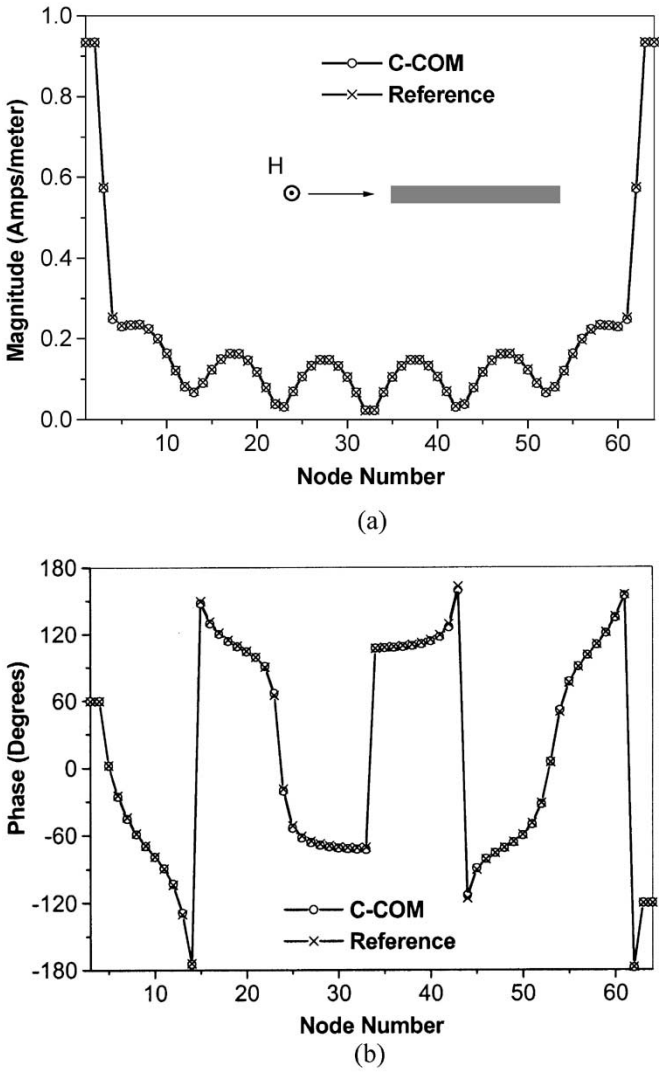

Fig. 12. Surface current density along the surface of a perfectly conducting slab for the case of end-on incidence, TE-polarization. Because of symmetry, only half of the surface span is considered. Node 3 corresponds to the middle of the left-hand-side surface. Nodes increase in number in the clockwise direction. (a) Magnitude and (b) phase.

only shown for field values on the upper half of the contour due to the symmetry of the solution. The results are presented for C-COM4(2,7) and the reference solution. For this and the following experiments, the reference solution is a reflection-free solution obtained when solving the problem in a domain large enough, while applying C-COM4(2,7), such that the boundary reflections are very small.

The same thin plate discussed above, measuring $0.2\ \lambda \times 3\ \lambda$, is studied under plane TE wave excitation. An identical computational geometry is used for both the scattering structure and computational domain. Unlike the results presented above where the field was plotted on an observation contour very close to the surface of the scatterer, here, we show the surface current density. Figs. 11 and 12 show the magnitude and phase of the surface current density for two different angles of incidence. Considering the close proximity of the perimeter of the computational domain from the scatterer, we observe a very strong agreement between the solution obtained using the C-COM and the reference solution. The strong performance of the C-COM solution is especially noticeable when scattered fields impinge at the computational boundary at or near grazing incidence.

For the two perfectly conducting scatterers chosen as representative geometry, the numerical results obtained show a very strong agreement between the C-COM solution and the reference solution. Such favorable agreement is achieved despite the very close proximity of the conductor to the outer boundary. The C-COM method also demonstrates effectiveness in predicting solutions with high degree of accuracy even when the solution is dominated by waves traveling at near-grazing incidence to the terminal boundary, as was the case for the end-on incidence in TM- and TE-polarization scattering.

V. Conclusion

This paper presented the extension of the C-COM theory for mesh truncation to the frequency-domain (time-harmonic) simulation of plane wave scattering by a perfect electric conductor.

The extension was made possible by implementing the concurrent averaging as a matrix operation. The application procedure was presented for the two-dimensional FDFD method. The extension to three-dimensional simulation follows in a similar fashion. Numerical experiments were presented validating the model and proving the robustness and accuracy of this mesh-truncation procedure. The strength of the C-COM method was especially demonstrated for waves incident at terminal boundaries at near grazing incidence. Highly satisfactory results obtained for all the numerical examples considered in this paper were obtained without any optimization of the algorithm used for the boundary operators. This proves the robustness of the C-COM for general radiation and scattering problems where no a priori knowledge is available on the nature of the scattered waves.

ACKNOWLEDGMENT

The authors would like to thank C. M. Rappaport for providing the FDFD-PML data used for comparison.

REFERENCES

[1] B. Engquist and A. Majda, "Radiation boundary conditions for the numerical simulation of waves," *Math. Comput.*, vol. 31, pp. 629–651, 1977.

[2] A. Bayliss and E. Turkel, "Radiation boundary conditions for wave-like equations," *Commun. Pure Appl. Math.*, vol. 23, pp. 707–725, 1980.

[3] G. Mur, "Absorbing boundary conditions for the finite-difference approximation of the time-domain electromagnetic-field equations," *IEEE Trans. Electromag. Comp.*, vol. 23, no. 4, pp. 377–382, Nov. 1981.

[4] R. L. Higdon, "Absorbing boundary conditions for acoustic and elastic waves in stratified media," *J. Comp. Phys.*, vol. 101, pp. 386–418, 1992.

[5] E. L. Lindman, "'Free-space' boundary conditions for the time dependent wave equation," *J. Comp. Phys.*, vol. 18, pp. 66–78, 1975.

[6] R. Mittra and O. M. Ramahi, "Absorbing boundary conditions for the direct solution of partial differential equations arising in electromagnetic scattering problems," in *Finite Element and Finite Difference Methods in Electromagnetic Scattering*, M. Morgan, Ed. New York: Elsevier Science, 1989, vol. 2, pp. 133–173.

[7] J.-P. Berenger, "A perfectly matched layer for the absorption of electromagnetic waves," *J. Comput. Phys.*, vol. 114, pp. 185–200, 1994.

[8] R. L. Higdon, "Radiation boundary conditions for dispersive waves," *SIAM J. Numer. Anal.*, vol. 31, no. 1, pp. 64–100, Feb. 1994.

[9] W. C. Chew and W. H. Weedon, "A 3D perfectly matched medium from modified Maxwell's equations with stretched coordinates," *Microwave Opt. Tech. Lett.*, vol. 7, no. 13, pp. 599–604, July 1994.

[10] O. M. Ramahi, "Complementary operators: A method to annihilate artificial reflections arising from the truncation of the computational domain in the solution of partial differential equations," *IEEE Trans. Antennas Propagat.*, vol. 43, pp. 697–704, July 1995.

[11] ——, "The Concurrent Complementary Operators Method for FDTD mesh truncation," *IEEE Trans. Antennas Propagat.*, vol. 46, pp. 1475–1482, Oct. 1998.

[12] ——, "Frequency-domain complementary operators for finite elements simulation," *IEEE Trans. Antennas Propagat.*, vol. 48, pp. 629–631, Apr. 2000.

[13] C. T. Law and X. Zhang, "Concurrent complementary operator boundary conditions for optical beam propagation," *IEEE Photon. Technol. Lett.*, vol. 12, pp. 56–58, Jan. 2000.

[14] O. M. Ramahi, "Concurrent Complementary Operators for mesh truncation in frequency-domain simulations," *IEEE Microwave Wireless Components Lett.*, vol. 12, pp. 99–101, Mar. 2002.

[15] X. Wu and O. M. Ramahi, "Application of the Concurrent Complementary Operators Method to numerically-derived absorbing boundary conditions," *Microwave Opt. Tech. Lett.*, vol. 32, no. 4, pp. 272–275, Feb. 2002.

[16] O. M. Ramahi, "Exact implementation of higher order Bayliss-Turkel absorbing boundary operators in finite-elements simulation," *IEEE Microwave Guided Wave Lett.*, vol. 8, pp. 360–362, Nov. 1998.

[17] A. Taflove and S. C. Hagness, *Computational Electrodynamics: The Finite-Difference Time-Domain Method*, 2nd ed. New York: Artech House, 2000.

[18] C. M. Rappaport, M. Kilmer, and E. Miller, "Accuracy considerations in using the PML ABC with FDFD Helmholz equation computation," *Int. J. Numer. Model*, vol. 13, no. 5, pp. 471–482, Sept.–Oct. 2000.

Omar M. Ramahi (S'86–M'90–SM'97) received the B.S. degree in mathematics and electrical and computer engineering (with highest honors) from Oregon State University, Corvallis, in 1984, and the M.S. and Ph.D. degrees in electrical and computer engineering from the University of Illinois at Urbana-Champaign, in 1986 and 1990, respectively.

From 1990 to 1993, he held a Visiting Fellowship position at the University of Illinois at Urbana-Champaign. From 1993 to 2000, he was with Digital Equipment Corporation (presently, Compaq Computer Corporation), where he was Member of the Alpha Server Product Development Group. In August 2000, he joined the Faculty of the James Clark School of Engineering, University of Maryland, College Park, where he is also a Faculty Member of CALCE Electronics Products and Systems Center. He was instrumental in developing computational techniques to solve a wide range of electromagnetic radiation problems in the fields of antennas, high-speed devices and circuits, and EMI/EMC. He was a Consultant to several companies and is a Cofounder of EMS-PLUS, LLC, and Applied Electromagnetic Technology, LLC. He has Authored and Coauthored more than 100 journal and conference papers and presentations. He is a coauthor of *EMI/EMC Computational Modeling Handbook* (Norwell, MA: Kluwer Academic, 1998). His research interests include experimental and computational EMI/EMC studies, high-speed devices and interconnects, biomedical applications of electromagnetics, novel optimization techniques, and interdisciplinary studies linking electromagnetic application with new materials.

Dr. Ramahi is a Member of the Electromagnetics Academy.

Vijaya Chebolu received the undergraduate degree from Osmania University, India, and the M.S. degree from the University of Maryland, College Park, in 2002.

Her fields of interest include electronic packaging, reliability, signal integrity, and electromagnetic compatibility. Her thesis, on numerical simulation of electromagnetic radiation and scattering problems, was based on research work conducted at the CALCE Electronic Products and Systems Center, University of Maryland.

Xin Wu was born in China in 1975. He received the B.E. degree from Tsinghua University, China, in 1996, the M.S. degree from the Chinese Academy of Sciences, in 1999, and the M.C.E. degree from The Johns Hopkins University, Baltimore, MD, in 2003. He is currently working toward the Ph.D. degree at the University of Maryland, College Park.

His research interests include computational electromagnetics and its applications in characterizing electronic packaging, high-speed interconnect modeling, and EMC/EMI.